Oxidation of Glycerol to Formaldehyde by Microsomes: Are Glycerol Radicals Produced in the Reaction Pathway?†

Julia Rashba-Step,‡ Eugene Step,§ Nicholas J. Turro,§ and Arthur I. Cederbaum*,‡

Department of Biochemistry, Mount Sinai School of Medicine, New York, New York 10029, and Department of Chemistry, Columbia University, New York, New York 10027

Received January 27, 1994; Revised Manuscript Received May 31, 1994®

ABSTRACT: Microsomes and reconstituted systems containing cytochrome P450 can oxidize glycerol to formaldehyde in a reaction catalyzed by an oxidant produced from the interaction of nonheme iron with H_2O_2. To evaluate the mechanism for this oxidation, the generation of glycerol radicals by various systems was compared to rates of formaldehyde production from glycerol. Photolysis of H_2O_2, oxidation of xanthine by xanthine oxidase in the presence of iron catalysts, or NADPH-dependent microsomal electron transfer in the presence of ferric–EDTA produced hydroxyl radicals. In the presence of glycerol these reaction systems produced DMPO–glycerol radical adducts which were detected by ESR spectroscopy. Despite the production of ·OH and glycerol spin-trapped adducts by these reaction systems, very low amounts or nondetectable amounts of formaldehyde were produced from the glycerol. However, significant amounts of formaldehyde were observed when microsomes were incubated in the presence of ferric ammonium sulfate or ferric–ATP, although ·OH production was lower with these iron catalysts than with ferric–EDTA. These results fail to support correlation between ·OH production and oxidation of glycerol to formaldehyde. Under conditions in which glycerol was oxidized to formaldehyde, no glycerol radical species could be observed with DMPO as the spin-trapping agent. These results suggest the oxidant (not ·OH) derived from the interaction of H_2O_2 with iron apparently cleaves glycerol to formaldehyde without the formation of a radical intermediate. Alternatively, the radical intermediate may be produced at a too low concentration to be detected or the radical intermediate may not be formed as a free species and therefore cannot be spin-trapped. By comparing microsomal rates of formaldehyde production from glycerol and glycerol-d_5, a kinetic isotope effect of about three was observed. The kinetic isotope effect was due to changes in V_{max} for formaldehyde production and not K_m for glycerol, suggesting that breakage of a carbon–hydrogen bond was a rate-determining step in the overall pathway of glycerol oxidation to formaldehyde.

Recent experiments with microsomes or reconstituted systems containing NADPH–cytochrome P450 reductase plus cytochrome P450 have shown that glycerol can be oxidized to formaldehyde by an oxidant produced from the interaction of nonheme iron with H_2O_2 (Clejan & Cederbaum, 1991, 1992a). Formaldehyde production from glycerol was inhibited by iron chelators such as desferrioxamine or EDTA or by removal of H_2O_2 by catalase or glutathione plus glutathione peroxidase. This reaction was not inhibited by superoxide dismutase or competitive hydroxyl radical (·OH)[1] scavengers nor by antioxidants such as Trolox, which block lipid peroxidation (Clejan & Cederbaum, 1991, 1992a,b). Besides glycerol, other vicinal glycols such as ethylene glycol, propane-1,2-diol, or butane 1,2-diol were also oxidized to formaldehyde by NADPH-dependent microsomal systems, whereas formaldehyde was not produced from geminal glycols such as propane-1,3-diol or butane-1,3- or -1,4-diol (Clejan & Cederbaum, 1992b). Since microsomes are often stored in glycerol-containing buffers, and glycerol is usually present as a stabilizer in preparations of cytochrome P450, NADPH–cytochrome P450 reductase, and other enzymes in high amounts, it appears important to be aware of circumstances by which glycerol can be oxidized by these systems and to understand the mechanism of this oxidation. The latter may be of value in use of formaldehyde production from glycerol as an assay for the presence of ferryl-type oxidants or oxidants (not ·OH itself) derived from the interaction of H_2O_2 with iron.

While previous experiments suggested that the oxidant responsible for glycerol oxidation to formaldehyde was not $O_2^{\cdot -}$, H_2O_2, or ·OH, the nature of the oxidizing species or whether the overall reaction pathway proceeds by formation of a glycerol radical is not known. The interaction of iron with H_2O_2 produces ·OH-like species as well as ferryl-type oxidants (Rush & Koppenol, 1986; Koppenol, 1985; Winterbourn & Sutton, 1986). Hydrogen abstraction from glycerol by ·OH or a ferryl-type oxidant should produce glycerol radicals, which can be detected by ESR spin-trapping experiments. To attempt to clarify the mechanism of glycerol oxidation to formaldehyde, the production of glycerol radicals by reactive oxygen intermediates generated by several different systems was compared to rates of glycerol oxidation to formaldehyde. The reaction systems were (a) photolysis of H_2O_2 which produces ·OH, (b) oxidation of xanthine by xanthine oxidase, which in the presence of iron catalysts, produces ·OH-like species, and (c) rat liver microsomes, which in the presence of iron catalysts, produces ·OH-like species and other oxidants which can oxidize glycerol to formaldehyde.

† This work was supported by USPHS Grants AA-09460 and AA-03312 from the National Institute on Alcohol Abuse and Alcoholism and by grants from The National Science Foundation.

* Address correspondence to this author at Department of Biochemistry, Box 1020, Mount Sinai School of Medicine, New York, New York 10029. Telephone: 212-241-7285. Fax: 212-996-7214.

‡ Mt. Sinai School of Medicine.

§ Columbia University.

® Abstract published in *Advance ACS Abstracts,* July 15, 1994.

[1] Abbreviations: $O_2^{\cdot -}$, superoxide anion radical; ·OH, hydroxyl radical or a speciesith the oxidizing power of the hydroxyl radical; ESR, electron spin resonance; DMPO, 5,5-dimethyl-l-pyrroline-*N*-oxide; KTBA, 2-keto-4-thiomethylbutyric acid.

0006-2960/94/0433-9504$04.50/0

It was considered that ESR spectroscopy would allow determination whether glycerol radicals are produced under conditions in which glycerol is oxidized to formaldehyde, and, if so, use of 1,3-[^{13}C]glycerol and [2-^{13}C]glycerol would identify on which carbon atom of glycerol the radical is produced or is most stable. Finally, the H/D kinetic isotope effect was also employed to determine if breakage of a carbon–hydrogen bond is a rate-limiting step in the overall pathway of oxidation of glycerol to formaldehyde and in the formation of glycerol radicals.

MATERIALS AND METHODS

Liver microsomes were isolated from male Sprague-Dawley rats weighing about 200 g. The rats were starved overnight prior to being killed. Animals were anesthetized with pentobarbital (150 mg/kg) and killed by decapitation. Liver homogenates (1:10) were prepared in 0.25 M sucrose, 0.01 M Tris, pH 7.4, and 0.001 M EDTA. Microsomes were isolated by differential centrifugation, washed twice, and resuspended in 0.125 M KCl and 0.01 M potassium phosphate, pH 7.4, and stored at −70 °C at a protein concentration of about 20 mg/mL. The production of formaldehyde from glycerol was routinely assayed in a reaction system containing 100 mM potassium phosphate, pH 7.4, 1 mM sodium azide (to inhibit any catalase present in the microsomes), 100 mM glycerol, and about 0.05–0.1 mg, of microsomal protein in a final reaction volume of 100 μL. Reactions were initiated by the addition of NADPH to a final concentration of 1 mM and were terminated after 30 min by addition of trichloroacetic acid to a final concentration of 6% w/v. After centrifugation to remove precipitated protein, the concentration of formaldehyde was determined on aliquots of the clear supernatant by the Nash reaction (Nash, 1953). The oxidation of 10 mM KTBA to ethylene gas by microsomes was determined in a similar reaction system except for replacing glycerol with KTBA and terminating reactions with HCl. Ethylene was determined by a head space, gas chromatography method (Cederbaum & Cohen, 1984).

The xanthine oxidase reaction system consisted of 100 mM potassium phosphate, pH 7.8, 0.14 mM xanthine, and 0.05–0.15 units of xanthine oxidase in a final volume of 0.5 mL. Substrates were either 100 mM glycerol or 10 mM KTBA. Most experiments were carried out in the presence of an iron catalyst, either 50 μM ferric–EDTA (1:2 iron/EDTA chelate) or 50 μM ferric ammonium sulfate. Reactions were initiated by the addition of xanthine oxidase and were carried out essentially as described for microsomal experiments.

Photolysis of H_2O_2 (usually 1 mM final concentration) to produce ·OH was carried out using the full light (water-filtered) of a 1000-W Xe–Hg lamp. For ESR experiments, the aqueous H_2O_2 solution was photolysed directly in the ESR cavity in the presence of 80 mM DMPO or 80 mM DMPO plus 100 mM glycerol for 1–5 min. To assay for the production of formaldehyde from 100 mM glycerol or ethylene from 10 mM KTBA, a steady-state photolysis of H_2O_2 was performed in a quartz cell for reaction periods ranging from 10 to 60 min. The Fenton reaction system consisted of an aqueous solution of 0.2–0.4 mM H_2O_2 mixed with 0.1 mM of freshly prepared ferrous ammonium sulfate.

ESR spectra were recorded in a W6-812Q flat quartz cell (Wilmad) on a Bruker E-300 spectrometer equipped with a 4102ST probe. The settings of the instrument were as follows: sweep width, 70.0 G; sweep time, 20.97 s; modulation amplitude, 0.5 G; modulation frequency, 100 kHz; microwave power, 11 mW. The spectra were recorded at room temperature (20–21 °C).

Table 1: Comparison of the Rate of Formaldehyde Production from Glycerol versus That of Hydroxyl Radical Generation by Various Reaction Systems[a]

reaction system	ethylene production from KTBA (nmol)	formaldehyde production from glycerol
(A)		
photolysis of H_2O (15 min)	1.74	ND
photolysis of H_2O_2 (60 min)	12.05	20 nmol/(mL·60 min)
(B)		
xanthine oxidase–$FeNH_4SO_4$	0.42	ND
xanthine oxidase–ferric–EDTA	1.10	ND
(C)		
microsomes–$FeNH_4SO_4$	0.80	79 nmol/(mL·30 min)
microsome–ferric–EDTA	2.73	24 nmol/(mL·30 min)

[a] ND, not detectable (detection limit = 5 nmol of formaldehyde). The oxidation of 10 mM KTBA to ethylene was determined as an index for the production of ·OH-like species. Production of formaldehyde from 100 mM glycerol was determined by the Nash reaction. Reaction systems were (A) photolysis of 1 mM H_2O_2 for either 15 or 60 min, (B) oxidation of xanthine by xanthine oxidase in the presence of either 50 μM ferric ammonium sulfate or 50 μM ferric–EDTA for a 30-min reaction period, and (C) oxidation of NADPH by rat liver microsomes in the presence of either 50 μM ferric ammonium sulfate or 50 μM ferric–EDTA for 30 min.

The spin trap 5,5-dimethyl-1-pyrroline-1-oxide (DMPO) was purchased from Sigma (St. Louis, MO). DMPO was further purified by passage through charcoal (Buettner & Oberley, 1978). The purified DMPO did not give any ESR signal when scanned at concentrations of 100 mM. Glycerol (molecular biology grade) was also from Sigma and used as received. Glycerol-d_5 (98 atom % D), [2-^{13}C] glycerol, and [1,3-^{13}C] glycerol (99 atom % ^{13}C) were purchased from Isotec (Matheson, Miamisburg, OH). No impurities were detected in the [^{13}C]glycerol when checked by ^{1}H and ^{13}C NMR using a Bruker WM-250 NMR spectrometer.

RESULTS

Formaldehyde Formation from Glycerol and ·OH Formation. Initial experiments utilized three different systems to generate reactive oxygen intermediates, a photochemical system, an enzymatic system, and a microsomal electron transfer system. Two reaction assays were carried out, the generation of ethylene gas from KTBA as a measure of the production of ·OH-like species and the cleavage of glycerol to yield formaldehyde as a product. Photolysis in the presence of 1 mM H_2O_2 produced ·OH as shown by the generation of ethylene, 1.7 nmol for a 15-min reaction period and 12 nmol for a 60-min reaction period (Table 1). The greater than linear increase in ethylene production with time is probably due to an autocatalytic decomposition of H_2O_2 under these photolytic conditions. Similarly, the oxidation of xanthine by xanthine oxidase in the presence of an iron catalyst or NADPH-dependent microsomal electron transfer in the presence of iron catalysts generated ethylene from KTBA (Table 1). Ferric–EDTA was more effective than ferric ammonium sulfate in catalyzing production of ·OH-like species by xanthine oxidase and by microsomes. However, with microsomes, ferric ammonium sulfate was more effective than ferric–EDTA in catalyzing the oxidation of glycerol to formaldehyde (Table 1). Similar results were found with ferric–ATP as the iron catalyst (data not shown). Moreover, formaldehyde generation from glycerol could not be detected in the xanthine oxidase system irrespective of the iron catalyst and in the 15-min photochemical reaction system. Some formaldehyde was produced from glycerol in the 60-min photochemical reaction system. These results indicate that formaldehyde generation from glycerol cannot be correlated

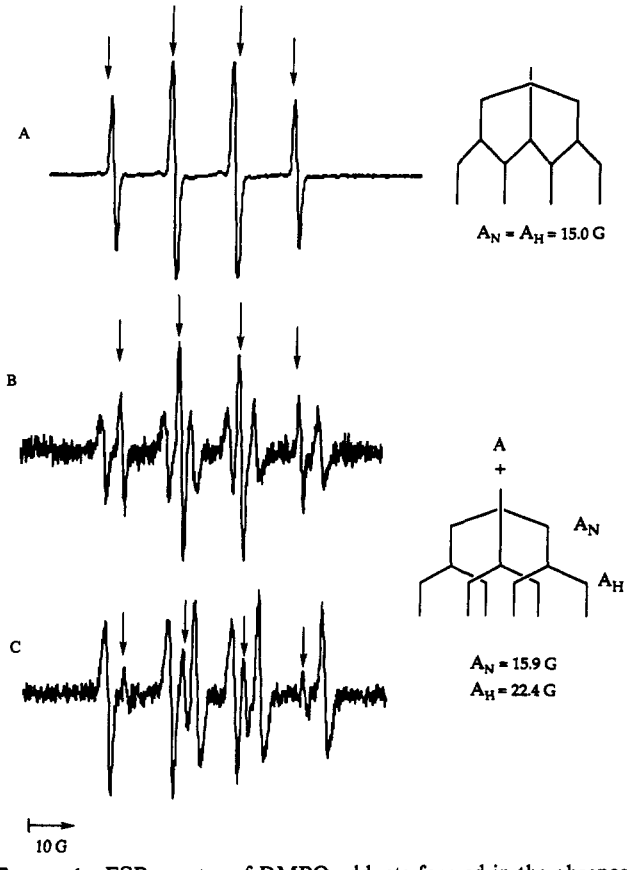

FIGURE 1: ESR spectra of DMPO adducts formed in the absence and presence of glycerol. (A) Photolysis of H_2O_2 in the presence of DMPO. (B) Photolysis of H_2O_2 in the presence of DMPO and 100 mM glycerol. (C) Oxidation of xanthine by xanthine oxidase in the presence of ferric–EDTA, DMPO, and 100 mM glycerol. Spectra A shows the four-line spectra characteristic of the DMPO–OH adduct, while spectra B and C show overlapping lines attributed to the DMPO–OH adduct (arrows) and DMPO–glycerol radical adduct.

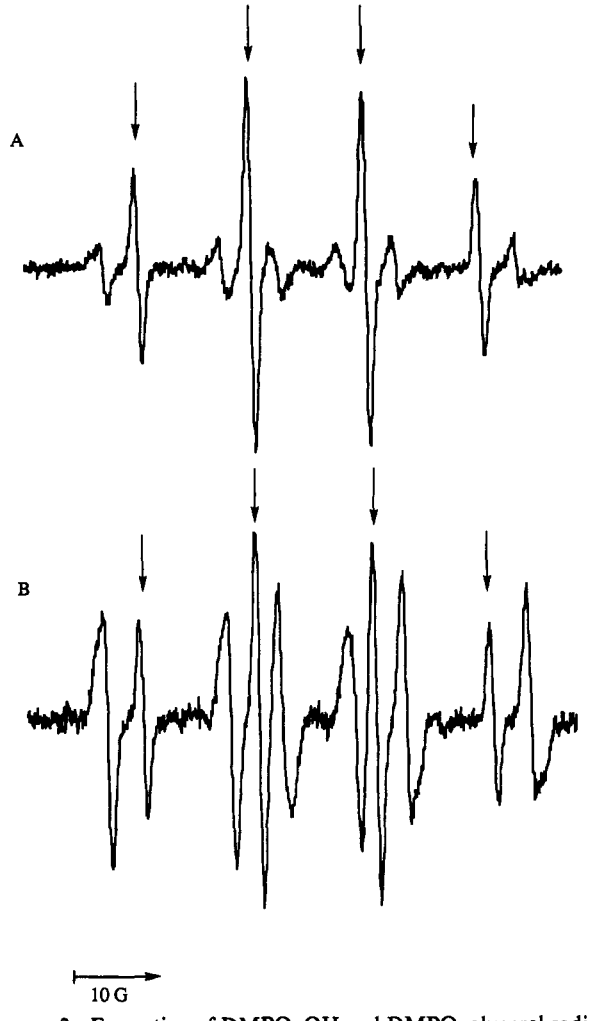

FIGURE 2: Formation of DMPO–OH and DMPO–glycerol radical adducts formed in a reaction system consisting of NADPH–cytochrome P450 reductase, NADPH, ferric–EDTA, DMPO, and either (A) 40 mM glycerol (the amount present in the reductase preparation) or (B) 100 mM added glycerol (total glycerol concentration of 140 mM).

with rates of ·OH production. It appears that microsomes can yield an oxidant produced from the interaction of H_2O_2 with iron which is effective in cleaving vicinal glycols to formaldehyde. ESR spin-trapping experiments were carried out to attempt to evaluate the overall mechanism for this reaction pathway.

DMPO–OH Adduct Formation. Photolysis of H_2O_2 in the presence of the spin-trapping agent DMPO gave rise to the four-line spectra of the DMPO-OH adduct (Figure 1A), with characteristic splitting constants $A_N = A_H = 15.0$ G (Lai & Piette 1978; Lai et al., 1979; Finkelstein et al., 1980). No adduct was observed in the absence of H_2O_2 or absence of photolysis. The Fenton reaction between H_2O_2 and ferrous ammonium sulfate gave rise to the same DMPO–OH signal as did photolysis of H_2O_2 (data not shown). Oxidation of xanthine by xanthine oxidase in the absence of added iron did not produce a DMPO–OH adduct; a weak signal was observed in the presence of ferric ammonium sulfate, and a more pronounced spectra was produced when ferric–EDTA was the iron catalyst (data not shown). Similar results were observed when NADPH was added to rat liver microsomes or purified NADPH–cytochrome P450 reductase, i.e., a DMPO–OH signal was found in the presence of ferric–EDTA.

DMPO–Glycerol Adduct Formation. When glycerol was added to the various reaction systems described for the detection of DMPO–OH adduct formation, a 10-line spectra was usually observed which appeared to reflect the overlapping of spectra of two different spin-trapped species, the four-line spectra of the DMPO–OH adduct and a six-line spectra ascribed to the adduct formed between DMPO with a carbon-centered glycerol radical. An example of such overlapping spectra for the photolysis of H_2O_2 in the presence of glycerol is shown in Figure 1B, while that for the xanthine oxidase reaction in the presence of ferric–EDTA plus glycerol is shown in Figure 1C. The splitting constants for the DMPO–glycerol adduct were $A_N = 15.9$ and $A_H = 22.4$ G. These splitting constants are similar to the splitting constants of other poly(ethylene glycol)–DMPO adducts (Samuni et al., 1986) and DMPO–carbon-centered radical adducts (Janzen & Haire, 1990; Mottley & Mason, 1989). The relative contributions of DMPO–OH and DMPO–glycerol adducts toward the overall signal were somewhat different for each reaction system, e.g., DMPO–OH was more prominent relative to DMPO–glycerol for the photolysis system than for the xanthine oxidase system. The contribution of the DMPO–glycerol signal increased, as expected, as the concentration of glycerol was elevated. Figure 2 compares the DMPO–OH and DMPO–glycerol adducts produced by NADPH–cytochrome P450 reductase in the presence of NADPH, ferric–EDTA, and either 40 mM (Figure 2A) or 140 mM (Figure 2B) glycerol. It should be noted that the 40 mM glycerol was the amount of glycerol present in the reductase preparation itself. The DMPO–glycerol adduct signal increased as the concen-

Scheme 1

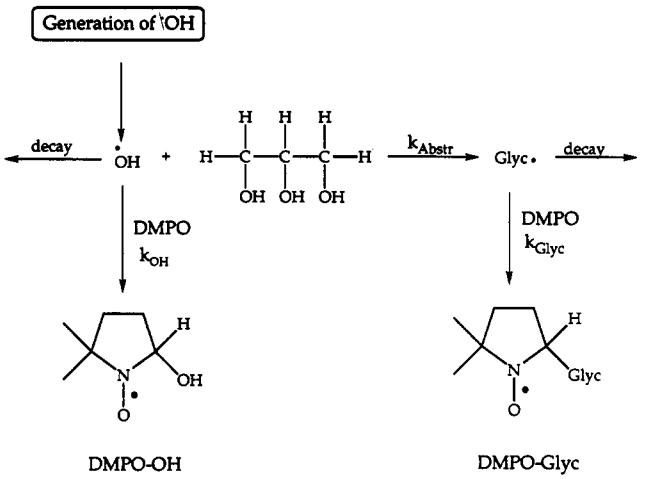

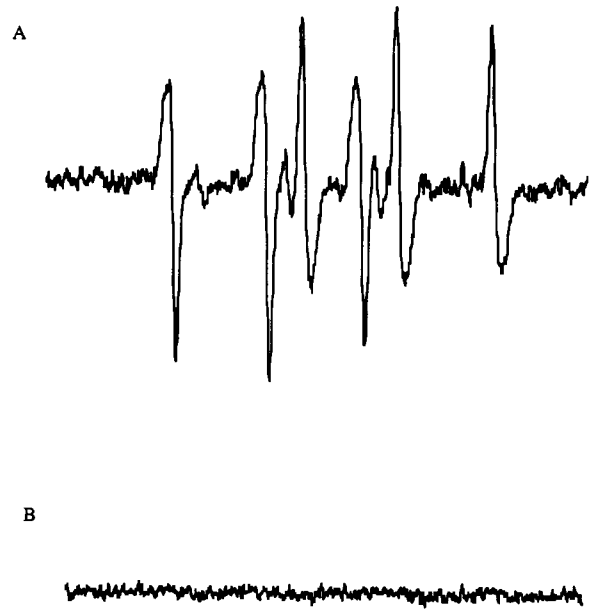

FIGURE 3: Comparison of the effectiveness of ferric–EDTA and ferric ammonium sulfate in stimulating the production of DMPO–OH and DMPO–glycerol radical adducts by the xanthine plus xanthine oxidase reaction system. (A) 50 μM ferric–EDTA, 30 scans; (B) 50 μM ferric ammonium sulfate, 30 scans.

tration of glycerol was elevated. Scheme 1 shows how the competition between scavenging of ·OH by DMPO to yield the DMPO–OH adduct and interaction of ·OH with glycerol to produce the DMPO-glycerol adduct promote formation of the DMPO–glycerol adduct over the DMPO–OH adduct as the concentration of glycerol increases.

The coupled oxidation of xanthine by xanthine oxidase in the presence of ferric–EDTA, DMPO, and glycerol gave rise to a prominent glycerol–DMPO adduct signal (Figure 3A). The intensity of this signal was decreased by 55–60% in the presence of 370 units/mL of superoxide dismutase and by 85% in the presence of 220 units/mL of catalase (data not shown). Ferric ammonium sulfate was ineffective relative to ferric–EDTA under these reaction conditions in catalyzing the production of DMPO–glycerol or DMPO–OH adducts (Figure 3B). When microsomes were incubated with glycerol, DMPO, NADPH, and ferric ammonium sulfate, conditions which result in significant formaldehyde production (Table 1), no glycerol–DMPO adducts could be observed, suggesting either the lack of formation of glycerol radicals by this system or their rapid decay or formation of spin-silent adducts.

Experiments with [^{13}C]Glycerol. To determine which C–H bond in glycerol is attacked by ·OH and what the structure of the ensuing glycerol radical is, experiments using 1,3-^{13}C- and 2-^{13}C-labeled glycerol were carried out. Additional splitting of the glycerol–DMPO signal would be expected when [^{13}C]glycerol radicals are produced in place of [^{12}C]glycerol radicals. The xanthine oxidase–ferric–EDTA reaction system was utilized for these experiments. With [2-^{13}C]glycerol as substrate, no additional splitting of the glycerol–DMPO signal was observed (Figure 4A) as compared with [2-^{12}C]glycerol (Figure 1C or Figure 3A for comparison). The contribution of the glycerol adduct with DMPO with [2-^{13}C]glycerol was smaller, while the DMPO–OH signal was larger than when [2-^{12}C]glycerol was the substrate. This may reflect a slightly lower rate constant for hydrogen abstraction by ·OH for [^{13}C]- versus [^{12}C]glycerol which results in an increase in the steady-state concentration of ·OH and subsequently in the DMPO–OH signal. Alternatively, the [2-^{13}C]glycerol DMPO spin adduct may be less stable.

Additional splitting was clearly observed with [1,3-^{13}C]-glycerol; the overall spectra is consistent with splitting of the glycerol-DMPO adduct into two lines (Figure 4B, compared to Figure 1C or Figure 3A or Figure 4A). It appeared that about 70% of the intensity of each line of the glycerol–DMPO adduct was split, whereas about 30% of the intensity of each line did not display additional splitting. Similar results were obtained in the H_2O_2 photolysis system as there was additional splitting of the glycerol–DMPO adduct signal with [1,3-^{13}C]-glycerol but not with [2-^{13}C]glycerol (data not shown).

Kinetic Isotope Effects on Glycerol Radical Formation and Production of Formaldehyde. To evaluate that breakage of a C–H bond is a rate-determining step in formation of glycerol radicals by ·OH abstraction, and whether such breakage is limiting in the overall pathway for cleavage of glycerol to formaldehyde, comparisons of rates with glycerol versus glycerol-d_5 were made. In the xanthine oxidase–ferric–EDTA system, the intensity of the DMPO–glycerol adduct after a 15-min reaction (70 scans accumulated) with glycerol was about twice that with glycerol-d_5 (data not shown). Since the line width of the glycerol-d_5 spin adduct was smaller than that of the glycerol spin adduct, the integrals of both spectra

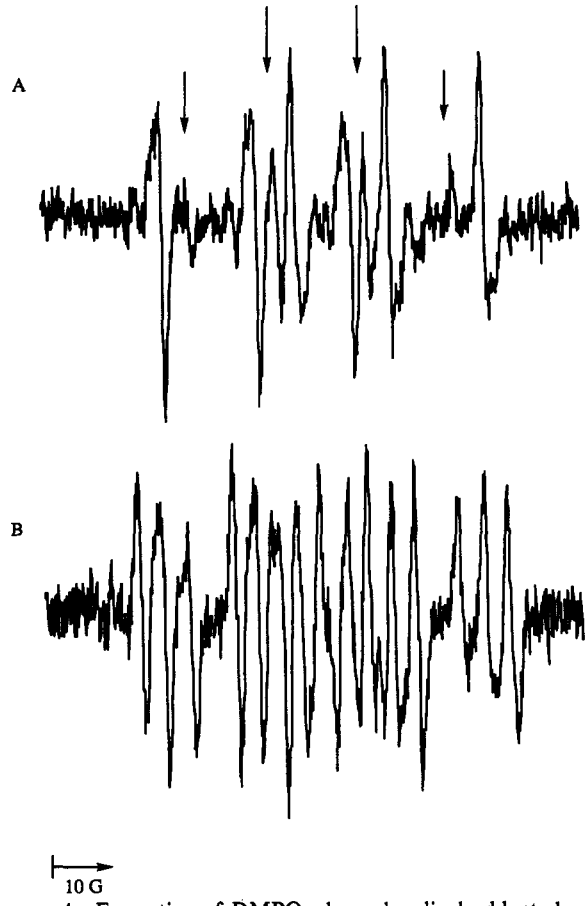

FIGURE 4: Formation of DMPO–glycerol radical adducts by the xanthine–xanthine oxidase–ferric–EDTA reaction system in the presence of either [2-^{13}C]glycerol, 30 scans (A), or [1,3-^{13}C]glycerol, 30 scans (B). Spectra are to be compared to those in Figure 1C or Figure 3A which utilized [^{12}C]glycerol.

were measured for quantitation of these signals. The integrals of the DMPO–glycerol adduct signals increased linearly over the interval of 3–20 min for both the deuterated and nondeuterated glycerol. The ratio of the spectra integrals of the spin adduct of DMPO with glycerol to DMPO–glycerol-d_5, which was taken to reflect the kinetic isotope effect of hydrogen abstraction from glycerol by ·OH, was 2.5–3.0.

The H/D kinetic isotope effect for formaldehyde production from microsomal oxidation of glycerol was determined in the presence of ferric ammonium sulfate and varying concentrations of unlabeled glycerol and glycerol-d_5. Results in Figure 5 show a Lineweaver–Burk plot of the rate of formaldehyde production as a function of the concentration of either unlabeled glycerol or glycerol-d_5. In this experiment, the V_{max} for formaldehyde production was 2.95 nmol/(min·mg of microsomal protein) for unlabeled glycerol and 1.07 nmol/(min·mg of protein for glycerol-d_5. K_m values were identical (about 7 mM) for unlabeled glycerol and glycerol-d_5. Results for four different microsomal preparations are summarized in Table 2. V_{max} values were 2.5–4-fold higher with unlabeled glycerol compared to glycerol-d_5, while K_m values were similar. The overall kinetic isotope effect, expressed as the ratio V_{max}/K_m for glycerol divided by the ratio V_{max}/K_m for glycerol-d_5 was 3.15 ± 0.6 for these four preparations. We attempted to measure the kinetic isotope effect of formaldehyde formation in the H_2O_2 photolysis system; however, due to the lower rates of formaldehyde production by this system, as compared to the microsomes, the error in these measurements was too large to allow for accurate quantitative data.

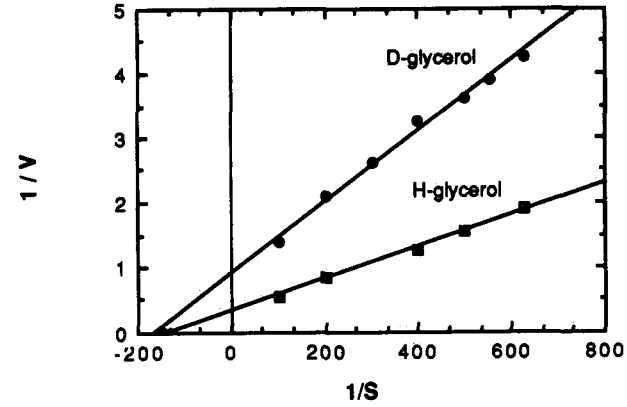

FIGURE 5: Lineweaver–Burk plot of the reciprocal of the rate of formaldehyde production by rat liver microsomes as a function of the reciprocal of the concentration of unlabeled glycerol or glycerol-d_5. The concentrations of glycerol utilized were 1.6, 2.0, 2.5, 3.3, 5, and 10 mM.

Table 2: Kinetic Isotope Effect for the Rate of Formaldehyde Production from Glycerol by Rat Liver Microsomes[a]

	V_{max}		K_m (mM)		kinetic
experiment	glycerol	glycerol-d_5	glycerol	glycerol-d_5	isotope effect
1	2.95	1.07	6.7	6.7	2.75
2	2.63	0.70	5.0	5.0	3.75
3	1.83	0.59	6.5	4.8	3.10
4	1.88	0.65	7.3	8.0	2.90

[a] The rate of formaldehyde production was determined as a function of various concentrations of either unlabeled glycerol or glycerol-d_5 (1.6–10 mM). Results were plotted as Lineweaver–Burk plots, and values for V_{max} [nmol/(min·mg of protein)] and K_m (mM) were determined for the two types of glycerol. The kinetic isotope effect was calculated as the V_{max}/K_m for unlabeled glycerol divided by V_{max}/K_m for glycerol-d_5. Results are from four different microsomal preparations.

DISCUSSION

Comparison of the rates of ·OH production as evaluated by formation of ethylene from KTBA or formation of glycerol spin-trapped adducts versus that of formaldehyde generation from glycerol indicates a lack of relationship between these two events. Rates of ethylene production from KTBA correlate well with formation of glycerol radicals by the various systems, e.g., increasing production of ethylene or glycerol radicals as a function of time of photolysis, or when ferric–EDTA is the iron catalyst in place of ferric ammonium sulfate in the xanthine oxidase or microsomal system. Glycerol oxidation to formaldehyde is readily observed with NADPH-dependent microsomal electron transfer in the presence of ferric ammonium sulfate, although this system is relatively weak as a producer of ·OH. We could not detect any production of formaldehyde from glycerol by the xanthine oxidase system. Some formaldehyde could be detected only after prolonged photolysis of H_2O_2, in which rates of ·OH production are more than an order of magnitude higher than that found with the microsomes. Yet even under these conditions of significant ·OH production, the production of formaldehyde is still considerably less than that catalyzed by the microsomes.

These results indicate that the oxidizing species derived from interaction of iron with H_2O_2, which oxidizes glycerol to formaldehyde is not ·OH. Under conditions in which microsomes actively oxidize glycerol to formaldehyde, we could not detect the presence of a glycerol–DMPO radical adduct which suggests that the overall reaction may proceed without detectable radical stages. Formation of glycerol radicals from the interaction of glycerol with ·OH could readily be detected

with DMPO. In the microsomal system, ferric–EDTA, which is superior to ferric ammonium sulfate as a catalyst for ·OH production, is, in fact, inferior as a catalyst for oxidation of glycerol to formaldehyde, suggesting competition between ·OH-mediated hydrogen abstraction radical, and nonradical (or perhaps masked-radical) pathways for oxidizing glycerol. The oxidant derived from the interaction of H_2O_2 with iron apparently cleaves glycerol without the formation of a radical intermediate or at least formation of such an intermediate in sufficient concentration to be detected by the spin-trapping technique. Sugimoto et al. (1987) have demonstrated that ferric chloride plus H_2O_2 in dry acetonitrile cause oxidative cleavage of vicinal diols to aldehydes by a mechanism involving the concerted removal of the two diol hydrogen atoms to produce a dioxetane intermediate, followed by homolytic cleavage to the aldehydes.

The kinetic isotope effect for formation of the DMPO–glycerol spin adduct or for the microsomal oxidation of glycerol to formaldehyde is about 3, suggesting that cleavage of a carbon–hydrogen bond is a rate-limiting factor in both reaction pathways of glycerol oxidation. The experimentally identical value for the two reactions suggests the possibility of similar structures of the transitional states of the rate-limiting steps for the two reactions. Since formation of the DMPO–glycerol adduct takes place after the primary hydrogen abstraction from glycerol by ·OH, it would be reasonable to assume that a determining step in the oxidation of glycerol to formaldehyde should also be hydrogen atom abstraction. Lack of detection of a glycerol–DMPO adduct may be due to the possibility that the primary glycerol radical is not formed as a free species and therefore cannot be spin-trapped. Interaction of the iron–H_2O_2 derived oxidant with glycerol, followed by primary hydrogen abstraction or transfer and eventually formaldehyde generation, may take place within the primary solvent cage or enzyme center. In this respect, previous experiments showed that cytochrome P450 was required for significant rates of formaldehyde production from glycerol (Clejan & Cederbaum, 1992a, 1993), even when potent redox cycling agents such as paraquat were added to microsomes or reconstituted systems. Since rates of oxidation of glycerol to formaldehyde by microsomes far exceed rates by other model chemical or enzymatic systems (Table 1), it is possible that P450 besides generating H_2O_2 and reducing nonheme iron, provides a favorable environment for this reaction to proceed. Such an environment (solvent cage or enzyme center) may allow for production of glycerol radicals which cannot be detected with DMPO and would be consistent with the results of Sugimoto et al. (1987) that a hydrophobic environment was necessary for cleavage of vicinals glycols by an iron–H_2O_2 system.

Experiments with [^{13}C]glycerol indicated that the glycerol radical spectra produced from the interaction of glycerol with ·OH displays further splitting when [1,3-^{13}C]glycerol, but not when [2-^{13}C]glycerol, is used. This is a surprising result and appears to suggest that hydrogen abstraction by ·OH occurs more readily with hydrogen atoms bound to carbon one than carbon two of glycerol. Such a result violates the conventional paradigms for the relative rates of hydrogen abstraction by radicals, so that other explanations for these results were sought. One such alternative explanation for the differential spectral pattern of the DMPO–glycerol adducts produced from [2-^{13}C]- and [1,3-^{13}C]glycerol is shown in Scheme 2. Reactions A and B show the expected glycerol radical which would be produced after hydrogen abstraction on carbon one or two, respectively. The boxes underneath the radical structure describe the expected splitting if [^{13}C]glycerol is used in place

Scheme 2

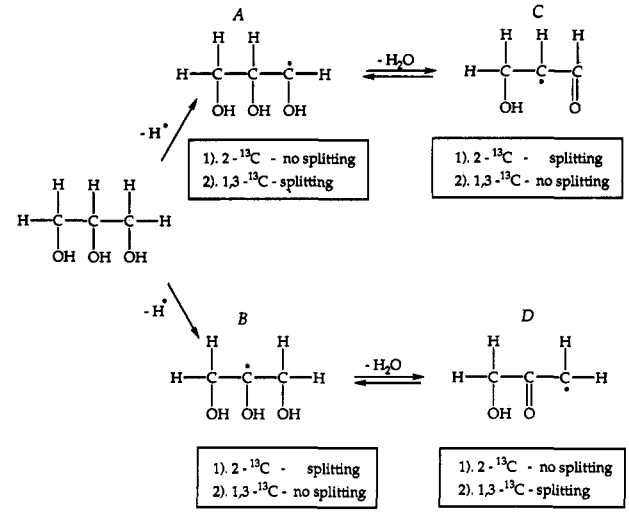

of [^{12}C]glycerol. Primary radicals which are the products of hydrogen abstraction from glycols, glycerol, and other polyols can be unstable in aqueous solution (Akhrem et al., 1993; Davies & Gilbert, 1991; Gilbert et al., 1972; Steenken et al., 1974, 1986). Such radicals, especially in acidic or basic aqueous solutions, can rearrange to produce secondary radicals, with migration of the radical center to the next carbon atom. For example, radical A can rearrange to structure C, while radical B can rearrange to structure D. Structures A and D are consistent with the ^{13}C-splitting data obtained for DMPO–glycerol adducts under our reaction conditions. Recent pulse radiolysis time-resolved experiments of glycerol in aqueous solution (pH ~ 7) with spin-echo detection showed that radical A is stable at neutral pH within the detection time interval (about 1 μs), while radical B is rearranged rapidly (within a few hundred of nanoseconds) to secondary radical D (private communication, Dr. Eli Shkrob, Argonne National Laboratory, IL). Therefore, it is likely that the DMPO–glycerol spin-trapped adducts shown in experiments of Figure 4 reflects a superposition of structures A and D, with a minor contribution of unstable structure B.

In summary, these results demonstrate that ·OH is not likely to play an important role in the overall pathway of microsomal oxidation of glycerol to formaldehyde. Breakage of a carbon–hydrogen bond is a rate-determining step in the overall pathway. The formation of glycerol radicals in this mechanism cannot be detected by ESR spectroscopy, suggesting that either the reaction proceeds without any detectable radical stage or, if produced, the radical intermediate cannot be detected because of too low a concentration or because it is not formed as a free species. Further studies are required to identify the overall mechanism for this pathway, nevertheless, the wide use of glycerol in studies with microsomes and cytochrome P450 suggest that awareness of this reaction may be important. The production of formaldehyde from glycerol may be of value in assays of potent oxidants derived from the interaction of iron with H_2O_2 in such mixed-function oxidase systems.

ACKNOWLEDGMENT

We thank Dr. Liviu Clejan for providing NADPH–cytochrome P450 reductase and Ms. Lucy Martinez for typing the manuscript.

REFERENCES

Akhrem, A. A., Kisel, M. A., Shadyro, O. I., & Yurkova, I. L. (1993) *Dokl. Phys. Chem. (Engl. Transl.)* *330*, 302–304.

Buettner, G. R., & Oberley, L. W. (1978) *Biochem. Biophys. Res. Commun. 83,* 69–74.
Cederbaum, A. I., & Cohen, G. (1984) *Methods Enzymol. 105,* 516–522.
Clejan, L. A., & Cederbaum, A. I. (1991) *Arch. Biochem. Biophys. 285,* 83–89.
Clejan L. A., & Cederbaum, A. I. (1992a) *FASEB J. 6,* 765–770.
Clejan, L. A., & Cederbaum, A. I. (1992b) *Arch. Biochem. Biophys. 298,* 105–113.
Clejan, L. A., & Cederbaum, A. I. (1993) *Biochem. J. 295,* 781–786.
Davies, M. J., & Gilbert, B. C. (1991) in *Advances in Detailed Reaction Mechanisms,* Vol. 1, pp 35–81, JAI Press, Greenwich, CT.
Finkelstein, E., Rosen, G. M., & Rauckman, E. T. (1980) *Arch. Biochem. Biophys. 200,* 1–16.
Gilbert, B. C., Larkin, J. P., & Norman, R. O. C. (1972) *J. Chem. Soc., Perkin. Trans. 2,* 794–802.
Janzen, E. G., & Haire, D. L. (1990) in *Advances in Free Radical Chemistry,* Vol. 1, pp 253–295, JAI Press, Inc., Greenwich, CT.
Koppenol, W. H. (1985) *J. Free Radicals Biol. Med. 1,* 281–285.
Lai, C. S., & Piette, L. H. (1978) *Arch. Biochem. Biophys. 190,* 27–38.
Lai, C. S., Grover, T. A., & Piette, L. H. (1979) *Arch Biochem. Biophys. 193,* 373–378.
Mottley, C., & Mason, R. P. (1989) in *Spin Labeling. Theory and Applications* (Berliner, L. J., & Reuben, J., Eds.) pp 489–546, Plenum Press, New York.
Nash, T. (1953) *Biochem. J. 55,* 416–421.
Rush, J. D., & Koppenol, W. H. (1986) *J. Biol. Chem. 261,* 6730–6733.
Samuni, A., Carmichael, A. J., Russo, A., Mitchell, J. B., & Riesz, P. (1986) *Proc. Natl. Acad. Sci. U.S.A. 83,* 7593–7597.
Steenken, S., Behrens, G., & Schulte-Frohlinde, D. (1974) *Int. J. Radiat. Biol. 25,* 205–210.
Steenken, S., Davies, M. J., & Gilbert, B. C. (1986) *J. Chem. Soc., Perkin Trans. 2,* 1003–1010.
Sugimoto, H., Spencer, L., & Sawyer, D. T. (1987) *Proc. Natl. Acad. Sci. U.S.A. 84,* 1731–1733.
Winterbourn, C. C., & Sutton, H. C. (1986) *Arch. Biochem. Biophys. 244,* 27–34.